CONVECTIVE AND NONCONVECTIVE ION BEAM FILAMENTATION INSTABILITIES

Richard F. Hubbard
Jaycor

ABSTRACT

The electromagnetic filamentation instability is expected to occur in heavy ion beam fusion target chambers. For a converging beam, the instability is expected to be convective with group velocity v_g approaching the beam velocity V_b until the beam is ~10-50 cm from the target. The number of e-foldings N_γ is estimated by integrating the local growth rate along the beam trajectory. For a cold beam, the result agrees with the initial value problem solution of Lee, et al. Detailed numerical solutions to the full dispersion region predict somewhat lower values for N_γ. Close to the target, $v_g \rightarrow 0$, and the instability is effectively nonconvective, with N_γ proportional to the pulse length. If a realistic conductivity model is used ($\sigma \sim (Z_b/R)^2$), the number of e-foldings in the nonconvective region is generally smaller than N_γ in the convective region. Thus, any appreciable deterioration in beam quality is more likely to occur while the beam is in the convective region.

I. INTRODUCTION

The electromagnetic filamentation instability may play an important role in determining allowable operating parameters for heavy ion fusion (HIF) systems. If allowed to grow to large amplitudes in the target chamber, self-magnetic fields arising from this instability would cause the ion beam to break into several self-pinched filaments or beamlets, possibly resulting in an unacceptable deterioration in beam focussing quality.

Theoretical analyses of this effect have attempted to predict the number of e-foldings N_γ of the electromagnetic field amplitudes using linear stability theory. Hubbard and Tidman[1] and Hubbard, et al[2] estimated N_γ based on a local dispersion relation (hereafter referred to as the "local approximation") which showed that for ballistic focussing systems, transverse beam heating reduced N_γ to acceptable levels ($N_\gamma \lesssim 5$) in most cases appropriate to HIF reactors. However, calculations by Lee, and his co-workers[3,4,5] which treated perturbations as an initial value problem gave somewhat higher estimates of N_γ and led them to the conclusion that filamentation instability defocussing may not be easy to avoid.

Previous calculations with the local approximation centered on the regime where the axial group velocity v_g (measured in the <u>laboratory</u> frame) is much less than the beam velocity V_b. In this nonconvective regime, N_γ is proportional to the pulse length, and the perturbations do not propagate in the laboratory frame. In this note, we examine the convective instability ($v_g \approx V_b$) in more detail. Our conclusions can be stated as follows:

1. The local approximation predicts that $v_g \approx V_b$ when the conductivity is low. N_γ can then be estimated by integrating the growth rate $\gamma(z)$ along the beam trajectory. For a ballistically focussed beam, the resulting N_γ <u>agrees</u>

with the initial value method for a cold beam and is smaller by a constant factor 0.31 for a sufficiently warm beam. Detailed numerical solutions to the dispersion relation tend to lie midway between the warm and cold beam results.

2. The instability is almost always nonconvective when the beam is near the pellet for HIF systems with ballistic focussing. The group velocity increases monotonically with distance z' from the pellet.

3. The lower N_γ and the claim of nonconvective instability predicted by the local approximation[1,2] was due in a large part to assuming a constant σ throughout the target chamber. If a more realistic conductivity model is assumed, ($\sigma \sim R^{-2}$ where R is the beam radius), maximum nonconvective growth occurs at ~10-50 cm from the pellet, and the values of N_γ are comparable with (but usually somewhat smaller than) those occurring in the convective regime.

4. Both the local approximation and the initial value method thus predict $N_\gamma \gtrsim 5$ for highly stripped high current beams (e.g., charge state $Z_b \gtrsim 70$, beam particle current $\tilde{I}_b \gtrsim 2$ kA). However, we believe that macroscopic self-magnetic fields arising from the ion beam or from "knock-on" electrons are likely to lead to unacceptable ion orbit deflections in this regime. In particular, we recommend using H_2 or He at ~1 torr to reduce Z_b to ~20. In this regime, N_γ can be $\lesssim 2$ and filamentation can be avoided.

II. REVIEW OF FILAMENTATION MODELS

The local approximation[1,2] is based on the dispersion relation for electromagnetic waves generated by a shifted Maxwellian ($f \sim \exp(-(v_z - V_b)^2/2\Delta v_z^2 - v_\perp^2/2\Delta v_\perp^2)$) ion beam with beam plasma frequency ω_b, average velocity $V_b = \beta c$ and thermal velocity $\Delta v_\perp$ propagating in a resistive medium with scalar conductivity σ.

$$H(\vec{k};\omega) = 0 = k^2c^2 - \omega^2 + \omega_b^2 \left\{1 - \frac{V_b^2}{\Delta v_\perp^2}\left(1 + \xi_b Z(\xi_b)\right)\right\} - 4\pi i\omega\sigma \ . \qquad (1)$$

Here $\xi_b = (\omega - k_{//} V_b)/\sqrt{2}\ k_\perp \Delta v_\perp$, and $Z(\xi_b)$ is the plasma dispersion function. Except for the conductivity term, Eq. (1) agrees with Davidson, et al[6] in the $k_{//} = 0$ limit. An additional term proportional to $k_{//}$ is negligible in the regime we are examining. The unstable mode is purely growing ($\omega_r = 0$) for $k_{//} = 0$. Approximate solutions in the hot beam regime ($|\xi_b| << 1$) and cold beam regime ($|\xi_b| >> 1$) for $k_{//} = 0$ are

$$\gamma = \mathrm{Im}(\omega) \underset{|\xi_b| << 1}{=} \frac{c^2(k_0^2 - k_\perp^2)}{-i\eta + 4\pi\sigma} \ , \qquad (2a)$$

and

$$\gamma = \beta\omega_b \underset{|\xi_b| >> 1}{} \ . \qquad (2b)$$

Here,

$$k_0 = \omega_b V_b/\Delta v_\perp c \qquad (3)$$

is the maximum unstable wave number, and

$$\eta = \frac{k_0^2 c^2}{\sqrt{2}\, k_\perp \Delta v_\perp} \left(Z(\xi_b) + \xi_b\, Z'(\xi_b) \right) \tag{4a}$$

$$\eta \underset{|\xi_b| << 1}{=} i\sqrt{\frac{\pi}{2}}\, k_0^2 c^2 / k_\perp \Delta v_\perp \tag{4b}$$

$$\eta \underset{|\xi_b| >> 1}{=} 2i\, \omega_b \beta\, (k_\perp c / k_0 \Delta v_\perp)^2 \quad . \tag{4c}$$

Eq. (2b) is valid only when $\beta\omega_b >> 4\pi\sigma\ \Delta v_\perp/c)^2$.

The axial group velocity for $k_{//} = 0$ is

$$v_g = \frac{\partial \omega_r}{\partial k_{//}} = -\frac{\partial H}{\partial k_{//}} \Big/ \frac{\partial H}{\partial \omega_r} = \frac{\eta\, V_b}{\eta + 4\pi i\sigma} \tag{5}$$

Clearly, $v_g \approx V_b$ for $-i\eta >> 4\pi\sigma$, leading to convective instability, while for $-i\eta << 4\pi\sigma$, $v_g \to 0$, and the instability is effectively nonconvective. In the nonconvective regime, $N_{\gamma,\ hot}^{nc} = \bar{\gamma}(z')\ \tau_p$ where $\bar{\gamma}$ is the average growth rate at position z' (with respect to the pellet) and τ_p is the pulse length. Close to the pellet, $\Delta v_\perp$ and σ are both large, and $v_g \to 0$ over a wide range of system parameters.[2]

The initial value method[3,4,5] predicts that for ballistic focussing, field amplitude $A \approx (L/(L-z))^\alpha$ where L is the chamber radius, and

$$\alpha = 2Z_b \left(\frac{L}{R_0}\right) \left\{ \frac{1}{\beta\gamma_r} \left(\frac{\tilde{I}_b}{m_e c^3/e} \right) \frac{m_e}{m_b} \right\}^{1/2} \quad . \tag{6}$$

Here R_0 is the beam radius at entry (z = 0). The number of e-folding is thus

$$N_\gamma = 2Z_b \left(\frac{L}{R_0}\right) \left\{ \frac{1}{\beta\gamma_r} \left(\frac{I_b}{(m_e c^3/e)} \right) \frac{m_e}{m_b} \right\}^{1/2} \ell n \left(\frac{L}{L-z} \right) \tag{7a}$$

$$= \left(\frac{\omega_{bo} L}{c}\right) \ell n \left(\frac{L}{L-z}\right) \qquad (7b)$$

Here ω_{bo} is the beam plasma frequency at $z = 0$, and $\gamma_r = (1 - \beta^2)^{-\frac{1}{2}}$.

III. LOCAL APPROXIMATION IN THE CONVECTIVE REGIME

We can recover the Lee, et al result (Eq. (7)) to within a numerical factor if $v_g \to V_b$ and Z_b is constant. For $|n| >> 4\pi\sigma$, Eq. (2a) for a hot beam can be integrated to give

$$N^c_{\gamma,hot} \approx \frac{1}{V_b} \int_0^{z^*} dz' \gamma(z') = \sqrt{\frac{2}{\pi}} \frac{k_\perp}{V_b} \left(1 - \frac{k_\perp^2}{k_0^2}\right) \int_0^{z^*} dx \Delta v_\perp(z') \ , \tag{8}$$

where z* is the approximate position at which the instability becomes nonconvective. In the absence of scattering, the thermal spread $\Delta v_\perp(z')$ increases from its value $\Delta v_{\perp o} = \Delta v_\perp(z = 0)$ according to[1]

$$\Delta v_\perp(z) = \Delta v_{\perp o}(R_o/R(z)) = \Delta v_{\perp o} \, L/(L-z) \tag{9}$$

Noting that maximum growth occurs at $k_\perp = k_o/\sqrt{3}$, Eq. (8) can be integrated to give

$$N^c_{\gamma,hot} = \frac{2}{3} \sqrt{\frac{2}{3\pi}} \frac{k_o \Delta v_{\perp o}}{V_b} L \, \ell n \, (L/(L-z)$$

$$= 0.31 \, \frac{\omega_{bo} L}{C} \, \ell n \left(\frac{L}{L-z^*}\right) \tag{10}$$

Eq. (10) therefore reduces to the Lee, et al result (Eq. (7)) in the nonrelativistic limit except for the numerical factor 0.31.

In the cold beam limit, the same procedure gives exact agreement with the initial value method. Noting that for Z_b constant, $\gamma(z) = \beta\omega_{bo}(R_o/R)$ $= \beta\omega_{bo}(L/L-z)$, the growth rate is integrated as before to give

$$N^c_{\gamma,cold} = \frac{\omega_{bo} L}{c} \, \ell n \left(\frac{L}{L-z^*}\right) . \tag{11}$$

IV. CONVECTIVE VS. NONCONVECTIVE INSTABILITY FOR $\sigma \sim R^{-2}$

We have previously claimed[2] that even though Eq. (6) allows v_g to vary from 0 to V_b, typical HIF parameters give - $i\eta << 4\pi\sigma$, and $v_g << V_b$. This led us to conclude that nonconvective instability was the more important, and that N_γ^{nc} given by Eq. (10) was a reasonable estimate for the number of e-foldings. However, the calculations in Refs. 1 and 2 assumed that conductivity σ was constant everywhere in the target chamber. When values of σ appropriate near the pellet are used, $v_g << V_b$ almost everywhere in the chamber. However, for typical ballistic focussing systems, we expect from classical transport models[7,8] that σ is several orders of magnitude lower near the chamber wall than at the pellet. We expect the instability to be convective in this regime with $v_g \approx V_b$.

In the region where R(z) exceeds a few centimeters, σ is approximately linear with density n_e. Direct ionization by the beam probably predominates, so $\sigma \sim n_e \sim R^{-2}(z)$. If $\sigma = \sigma_0(R_0/R)^2 = \sigma_0(L/(L-z))^2$ is assumed everywhere, the position z* where the instability changes from convective to nonconvective is given by $\eta(z^*) \approx 4\pi\sigma(z^*)$, or

$$\sqrt{\frac{\pi}{2}}\ \frac{k_0^2 c^2}{\alpha\, k_0 (\Delta v_{\perp 0} L/(L-z^*))} = 4\pi\ \sigma_0 \left(\frac{L}{L-z^*}\right) \tag{12}$$

Here $\alpha \simeq 0.5 = k_\perp/k_0$. The boundary z* is thus

$$z^* = \left[1 - \left(\frac{4\sqrt{2\pi}\ \ \alpha\beta\sigma_0\Delta v_{\perp 0}}{V_b k_0 c}\right)^{1/3}\right] L \quad . \tag{13}$$

The situation is illustrated in Figure 1 which shows typical regions of convective and nonconvective instability. Since $\eta \sim R$ and $\sigma \sim R^{-2}$, the transition region where $v_g \sim \frac{1}{2} V_b$ is quite small. Eq. (13) predicts $(1 - z^*/L) \sim 0.05 - 0.1$ in most cases. For $\sigma \sim R^{-2}$ maximum growth actually occurs in the convective

regime where $\eta = 8\pi\sigma$ and $v_g = \frac{2}{3} V_b$. However, we expect that detailed beam transport code results to show that $\sigma(z)$ will probably increase faster than R^{-2} in the $z \simeq z^*$ region due to avalanching and then increase more slowly with R as the plasma becomes fully ionized near the pellet. Thus, maximum growth may well occur in the nonconvective regime.

The following scenario can therefore be constructed. In the convective regime, perturbations are carried along with the beam until they arrive at $z \simeq z^*$. The number of e-foldings N_γ^c accumulates according to Eq. (10) or (11). As the beam continues to propagate, perturbations are rapidly left behind as v_g becomes small. The number of e-foldings is then obtained by calculating $\gamma(z')$ from Eq. (2) and taking $N_\gamma^{nc} \simeq \gamma(z')\tau_p$. Filamentation defocussing will be determined by the larger of the two N_γ's.

As an example, consider a 2 kA, 20 GeV, 10 nsec Uranium beam with $Z_b = 20$, $\Delta v_{\perp o}/V_b = 10^{-4}$, R_o - 10 cm, $\sigma_o = 10^{12}$ s^{-1}, and L = 500 cm. Then $z^* \simeq 470$ cm, and $N_{\gamma,hot}^c = 1.4$. Note that $N_{\gamma,cold}^c = 3\ N_{\gamma,hot}^c$. The calculation of N_γ^{nc} is somewhat arbitrary since maximum growth does not occur in the nonconvective regime. If we choose $z = z^* + 0.2\ (L-z^*)$, then $v_g \sim 0.25\ V_b$, and $N_\gamma^{nc} \simeq 0.85$. $N_{\gamma,hot}^c > N_\gamma^{nc}$ in this example, but the difference is less than a factor of 2. If $Z_b = 70$ (which is typical of Ne at 1 torr instead of H_2 or He at 1 torr) then $z^* = 480$ cm, $N_{\gamma,hot}^c = 5.8$, and $N_\gamma^{nc} = 4.5$. We have calculated N_γ^c and N_γ^{nc} for a variety of HIF parameters; in most cases, $N_{\gamma,hot}^c > N_{\gamma,hot}^{nc}$ but the disagreement is usually less than a factor of 2. In general, $N_\gamma^{nc} > N_{\gamma,hot}^c$ can be obtained by increasing the ratio of the pulse length τ_p to the beam transit time $\tau_L = L/V_b$ or by changing the details of the conductivity model. The most dangerous nonconvective instability occurs at some tens of centimeters from the pellet where σ^{-1} (and hence N_γ^{nc}) may be an order of magnitude higher than the value near the pellet used by Hubbard, et al.[1,2]

Beam convergence does not play a role in the nonconvective regime, so one might expect approximate agreement with Lee's calculations for a non-converging finite-pulse beam.[3] For a warm beam of length τ_p, the number of e-foldings predicted by Lee is

$$N_{\gamma,hot} \leq (\xi_L^{-2} - 1) \frac{\tau_p}{\tau_m} , \tag{14}$$

where $\tau_m = k^2c^2/4\pi\sigma$, and $\xi_L^2 = k^2\Delta v_\perp^2 / \beta^2\omega_b^2$. (Note that he defines $\Delta v_\perp$ to be $\sqrt{2}$ larger than our value.) Substituting the definitions of τ_m and ξ_L gives

$$N_{\gamma,hot} \leq \left\{ \frac{\omega_b^2 \beta^2 c^2}{4\pi\sigma\Delta v_\perp^2} - \frac{k^2c^2}{4\pi\sigma} \right\} \tau_p \quad . \tag{15}$$

This upper limit agrees <u>exactly</u> with Eq. (2a) in the nonconvective limit ($4\pi\sigma >> - i\eta$).

V. NUMERICAL SOLUTIONS TO FILAMENTATION DISPERSION RELATION

Since the local approximation predicts that $N^c_{\gamma,hot}/N^c_{\gamma,cold} = 0.31$, independent of model parameters, we expect that numerical solutions to the full dispersion relation (Eq. (1)) will lie between the limits given by Eqs. (10) and (11). We have carried out such a calculation, numerically integrating solutions to Eq. (1) from $z = 0$ to $z = z^*$ as given in Eq. (13).

Figure 2 summarizes the results of such a calculation for a 1 kA Uranium beam with $Z_b = 18.1$ (He at 1 torr), $\beta = 0.4$, $\Delta v_\perp/V_b = 2 \times 10^{-4}$, $L = 5$ m, $R_o = 10$ cm, and $\sigma_o = 10^{11}$ s^{-1}. The figure plots the "exact" growth rate $\gamma_{ex}(z)$, accumulated e-foldings $N^c_{\gamma,ex}(z) \equiv \int_o^z dx\, \gamma_{ex}(x)/V_b$, and plasma dispersion function argument $|\xi_b(z)|$ verses distance z from the chamber wall. The value $k_\perp = 2.5$ cm$^{-1} \approx 2.5\, k_o$ was chosen to maximize $N^c_{\gamma,ex}(L-z^*) \equiv N^c_{\gamma,ex}$. Since $|\xi_b| \sim 1$, it is not surprising that $N^c_{\gamma,ex} = 2.0$ lies near the average of $N^c_{\gamma,hot} = 1.0$ and $N^c_{\gamma,cold} = 3.3$. Eq. (13) is usually adequate for estimating z^* since $|\xi_b(z = z^*)|$ is almost always less than 0.5; $z^* = 480$ cm for the above example. The rapid drop in γ and $|\xi_b|$ as $z \to L$ is seen in all ballistic mode propagation examples we have investigated.

Figure 3 plots $N^c_{\gamma,hot}$, $N^c_{\gamma,cold}$, and $N^c_{\gamma,ex}$ verses $k_\perp$ for the example in Figure 2. The variations in the analytical estimates of $N^c_{\gamma,cold}$ is entirely due to small changes in z^* as $k_\perp$ is changed. The peak in $N^c_{\gamma,ex}(k_\perp)$ is quite broad, and in all cases, $N^c_{\gamma,ex} \lesssim 0.6\, N^c_{\gamma,cold}$.

Figure 4 plots the three estimates of N^c_γ, the beam change state Z_b, and the convective - nonconvective boundary z^* verses pressure in torr assuming Helium in the target chamber. Z_b was estimated using a variation of the Yu, et al model,[7] and the calculation will be described in more detail elsewhere. We assume $\sigma_o = 3 \times 10^9\, Z_b^2$, which again comes from assuming that direct

ionization by the beam is the dominant process, and other parameters are as in Figure 2. $N^c_{\gamma,ex}$ is maximum for $k_\perp \sim 0.25\ k_o$ in all cases, and begins to look dangerous ($N^c_{\gamma,ex} \sim 5$) for $Z_b \gtrsim 50$. This high charge state is reached at much lower pressures (below 1 torr) for heavier gases such as Neon. Again, $N^c_{\gamma,ex}$ is almost a factor of two lower than $N^c_{\gamma,cold}$ in all cases.

Two factors which have been omitted from our analysis may further reduce $N^c_{\gamma,ex}$. First, the constant Z_b assumed was the upper limit calculated at z = L. Using a variable $Z_b(a) \leq Z_b(L)$ in the numerical integration would obviously reduce $N^c_{\gamma,ex}$ somewhat. Also, filamentation growth ceases for modes with $k_\perp \lesssim \pi/R(z)$ as the beam approaches the pellet since the unstable wavelength exceeds the beam diameter. At pressures below a few torr, this effect probably causes convective growth to cease before the beam reaches the convective/nonconvective boundary at $z = z^*$. For example, in the 1 torr case, the condition $R = \pi/k_\perp$ is reached at a distance z = 450 cm from the wall for $k_\perp$ = 3 cm which is smaller than z^* = 479cm. $N^c_{\gamma,ex}(z = 450\ cm)$ is only 1.8 instead of our earlier estimate of 2.0. The two effects cited here may reduce N^c_γ by as much as a factor of two at low pressures; the reduction is much smaller for $Z_b \gtrsim 50$ or higher beam currents. The dotted line in Figure 4 shows the effect of cutting off $N^c_{\gamma,ex}$ when the unstable wavelength exceeds R(z). The dashed line gives an estimate of the nonconvective number of e-foldings N^{nc}_γ, which is always less than $N^c_{\gamma,ex}$ for a 10 nsec pulse.

V. CONCLUSIONS

The local dispersion relation for the electromagnetic filamentation instability predicted to occur in heavy ion fusion target chambers will be convective until the beam is a few tens of centimeters from the target. Upper and lower limits on the number of e-foldings of the field amplitudes (N_γ^c) in the convective regime are given by Eqs. (10) and (11) for ballistically focussed beams. Numerical integration along the beam trajectory of the full dispersion relation solutions (Eq. (1)) give estimates of $N_{\gamma,ex}^c$ which are near the average of the upper and lower limits. Close to the pellet, the instability is effectively nonconvective, and the results of Hubbard and Tidman[1] generally apply. However, N_γ^{nc} is usually lower than N_γ^c, and hence the most serious deterioration of beam quality will usually occur in the convective regime.

The calculation by Lee for ballistic mode filamentation is assumed $|\xi_b| \gg 1$, and the local approximation agrees <u>exactly</u> with Lee's result in this cold beam limit. However, numerical solutions to Eq. (1) indicate that $|\xi_b| \sim 1$ in most cases, leading to estimates of $N_{\gamma,ex}^c$ which are somewhat lower. The inclusion of a variable beam charge state will further reduce $N_{\gamma,ex}^c$, as will cutting off N_γ at the point where the beam radius becomes less than the unstable wavelength. Thus, the local approximation leads to the same scaling as the method of Lee, et al[3,4,5], but our detailed numerical estimates of the number of e-foldings are typically a factor of two lower. Also, the local approximation agrees with Lee's method in the high conductivity (nonconvective) limit in which N_γ is proportional to the pulse length.

Fig. 4 indicates that the most promising way of controlling filamentation growth is to minimize the beam charge state Z_b. For a variety of reasons, recent reactor scenarios have involved somewhat lower beam energies ($\sim$10 GeV), higher currents, and heavier gases (e.g., Neon). This will make it difficult, if not impossible, to keep Z_b low unless the chamber pressure is lowered significantly . The higher beam densities associated with these scenarios further increase filamentation growth rates for the ballistic propagation mode in $\sim$1 torr gas-filled reactors. However, both pinched-mode propagation in gas-filled reactors and ballistic mode propagation in low density ($< 10^{-3}$ torr) Lithium waterfall reactors are much less susceptible to filamentation instability and may have other important advantages as well.

ACKNOWLEDGEMENTS

Conversations with Drs. Derek Tidman, John Guillory, Paul Ottinger, and E. Lee are gratefully acknowledged. This work was supported by the Department of Energy under contract DE-AC08-79-DP40101.

REFERENCES

1. R. F. Hubbard and D. A. Tidman, Phys. Rev. Lett. 41, 866 (1978).

2. R. F. Hubbard, D. S. Spicer, and D. A. Tidman, in Proceedings of the Heavy Ion Fusion Workshop, Argonne National Laboratory, p. 379 (1978).

3. E. P. Lee, in Ref. 2, p. 393; E. P. Lee, Bull. Am. Phys. Soc. 23, 888 (1978).

4. F. W. Chambers, E. P. Lee, and S. S. Yu, Bull. Am. Phys. Soc. 23, 770 (1978).

5. H. L. Buchanan, F. W. Chambers, E. P. Lee, S. S. Yu, R. J. Briggs, and M. N. Rosenbluth, Lawrence Livermore Laboratory, UCRL Report 82586, 1979.

6. R. C. Davidson, D. A. Hammer, I. Haber, and C. E. Wagner, Phys. Fluids 15, 317 (1972).

7. D. S. Spicer, R. F. Hubbard, and D. A. Tidman, Bull. Am. Phys. Soc. 23, 770 (1978).

8. S. S. Yu, H. L. Buchanan, E. P. Lee, and F. W. Chambers, Ref. 2, p. 403.

LIST OF SYMBOLS

$H(\vec{k};\omega)$	Plasma dielectric function
$k_\perp$, $k_{//}$	Perpendicular and Parallel wavenumbers
$\omega = \omega_r + i\gamma$	Frequency
V_b	Beam velocity
$\Delta v_\perp$	Transverse beam thermal velocity
$Z(\xi_b)$	Plasma dispersion function with argument $\xi_b = (\omega - k_{//} V_b)/\sqrt{2}\, k_\perp \Delta v_\perp$
σ	Electrical conductivity
ω_b	Beam plasma frequency
$Z'(\xi_b)$	$dZ(\xi_b)/d\xi_b$
η	See Equation (4)
v_g	Parallel group velocity
τ_p	Pulse length (temporal)
Z_b	Beam charge state
L	Chamber radius
z	Distance from the chamber wall
N_γ	Number of e-foldings of e-m field
N_γ^{nc}	Nonconvective number of e-folds
$N_{\gamma,hot}^{c}$	Convective number of e-folds, $\lvert\xi_b\rvert \ll \lvert$
$N_{\gamma,cold}^{c}$	Convective number of e-folds, $\lvert\xi_b\rvert \gg \lvert$
$N_{\gamma,ex}^{c}$	Convective number of e-folds, numerical solution to full plasma disp. relation

R	Beam radius
R_o, ω_{bo}	Values at injection
z^*	Location of transition between convective and nonconvective regions ($v_g = \frac{1}{2} V_b$)
$\tilde{I}_b$	Beam <u>particle</u> current

FIGURE CAPTIONS

Figure 1. Approximate locations of the convective and nonconvective regions of filamentation instability for a ballistically focussed heavy ion beam. For most of the beam trajectory, the group velocity $v_g \approx V_b$, the beam velocity, so perturbations are convected with the beam. However, close to the target, v_g decreases rapidly due to an increase in conductivity and transverse beam temperature. Perturbations pile up locally, and the instability is effectively nonconvective. The transition between the two regions is defined by the position z^* at which $v_g = \frac{1}{2} V_b$.

Figure 2. Filamentation growth rate γ, number of e-foldings $N^c_{\gamma,ex}(z)$, and plasma dispersion function argument $|\xi_b| = \gamma/\sqrt{2}\, k_\perp \Delta v_\perp$, plotted verses distance z from the chamber wall. We assume a 20 GeV Uranium beam with charge $Z_b = 18$, $\tilde{I}_b = 1$ kA, initial radius $R_o = 10$ cm, $\Delta v_{\perp o}/V_b = 2 \times 10^{-4}$, L = 5 meters, $k_\perp = 0.25\, k_o = 2.5\ \text{cm}^{-1}$, and $\sigma = 10^{11} (R_o/R)^2\ \text{sec}^{-1}$. The growth rate is calculated numerically using the full dispersion relation (Eq. (1)), and $N^c_{\gamma,ex}(z) = V_b^{-1} \int_o^z \gamma(z')\, dz'$ is integrated only up to the transition point z^* defined by Eq. (13). Since $|\xi_b| < 2.6$ everywhere, $N^c_{\gamma,ex}$ is substantially below the $|\xi_b| \gg 1$ cold beam limit.

Figure 3. Variation of the three estimates of N^c_γ based on Equations (1), (8), and (11), verses $k_\perp/k_o$, where $k_o = \omega_b V_b/\Delta v_\perp c$ is independent of z if Z_b is constant. All other parameters are as in Figure 2. The small variation in $N^c_{\gamma,cold}$ is entirely due to changes in z^* with $k_\perp$. The exact numerical solution $N^c_{\gamma,ex}$ has a broad peak centered on $k_\perp = 0.25\, k_o$ which lies near the average of the cold and hot beam

analytical estimates. The cold beam estimate agrees with the Lee, et al results for a converging beam.

Figure 4. Beam charge state Z_b, location z* of the convective-nonconvective transition region, and the three estimates of N_γ^c as functions of the chamber pressure in torr, assuming Helium. The increase in the number of e-foldings with pressure is due entirely to the increased beam charge state, which increases both ω_b and σ. The dotted line shows the effect of cutting off the integration of N_γ^{ex} at the point where the unstable wavelength exceeds the beam radius. The dashed line is an estimate of N_γ^{nc} taken slightly into the nonconvective regime. The variation of N_γ^{nc} with pressure is reduced considerably by assuming $\sigma \sim Z_b^2$. Note that $N_\gamma \gtrsim 5$ is considered dangerous.

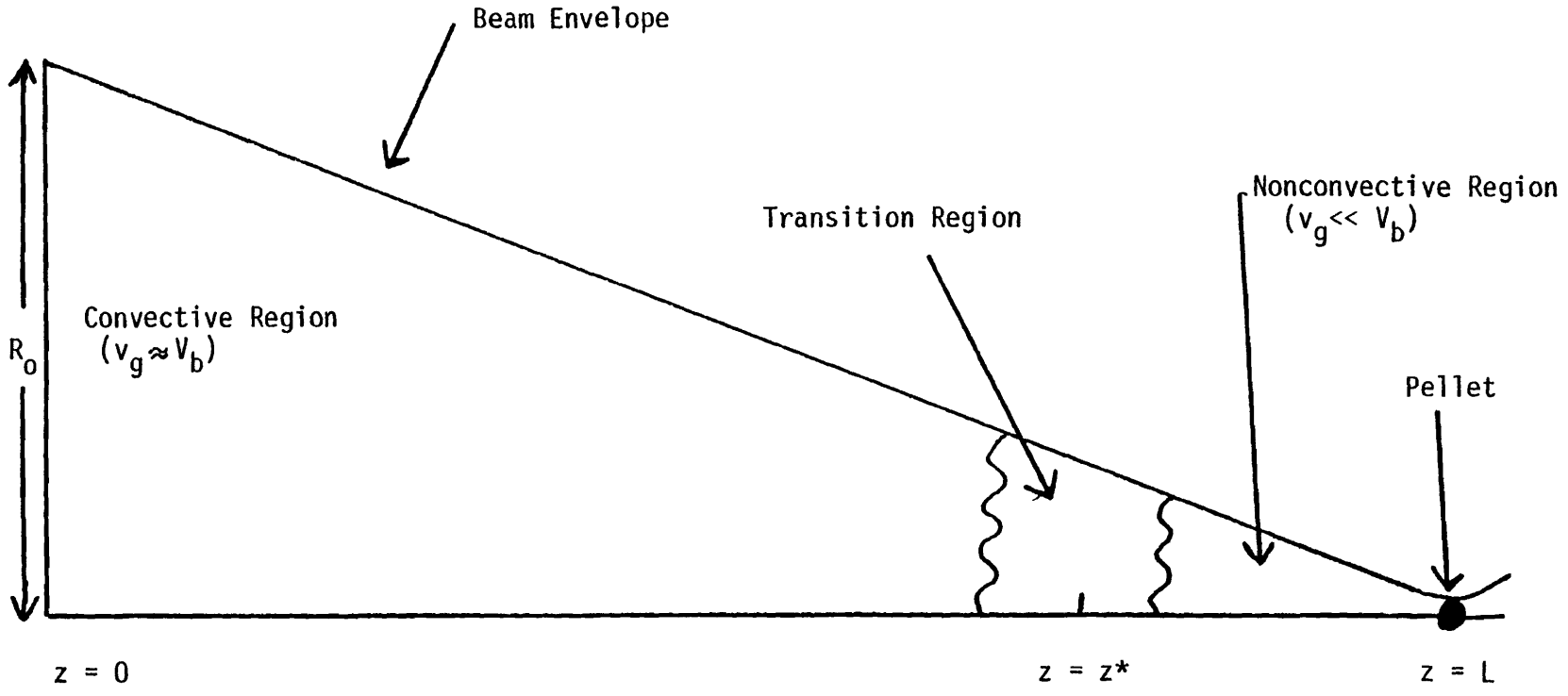
Beam Envelope
Transition Region
Nonconvective Region
($v_g << V_b$)
Convective Region
($v_g \approx V_b$)
R_o
Pellet
z = 0
z = z*
z = L

Figure 1

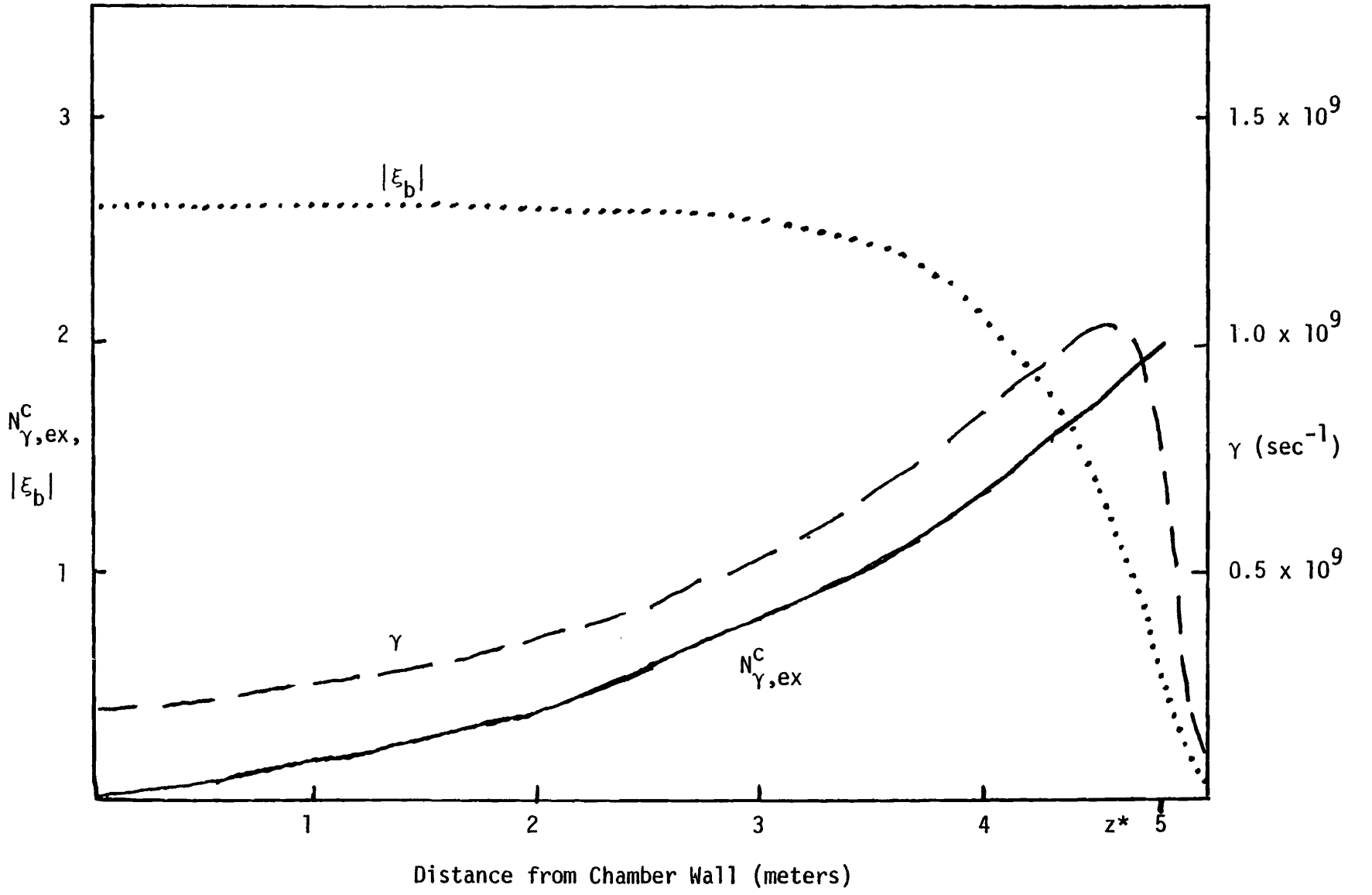
3
2
1
$N^C_{\gamma,ex}$,
$|\xi_b|$
$|\xi_b|$
γ
$N^C_{\gamma,ex}$
1.5 x 10^9
1.0 x 10^9
0.5 x 10^9
γ (sec^{-1})
1
2
3
4
z*
5
Distance from Chamber Wall (meters)

Figure 2

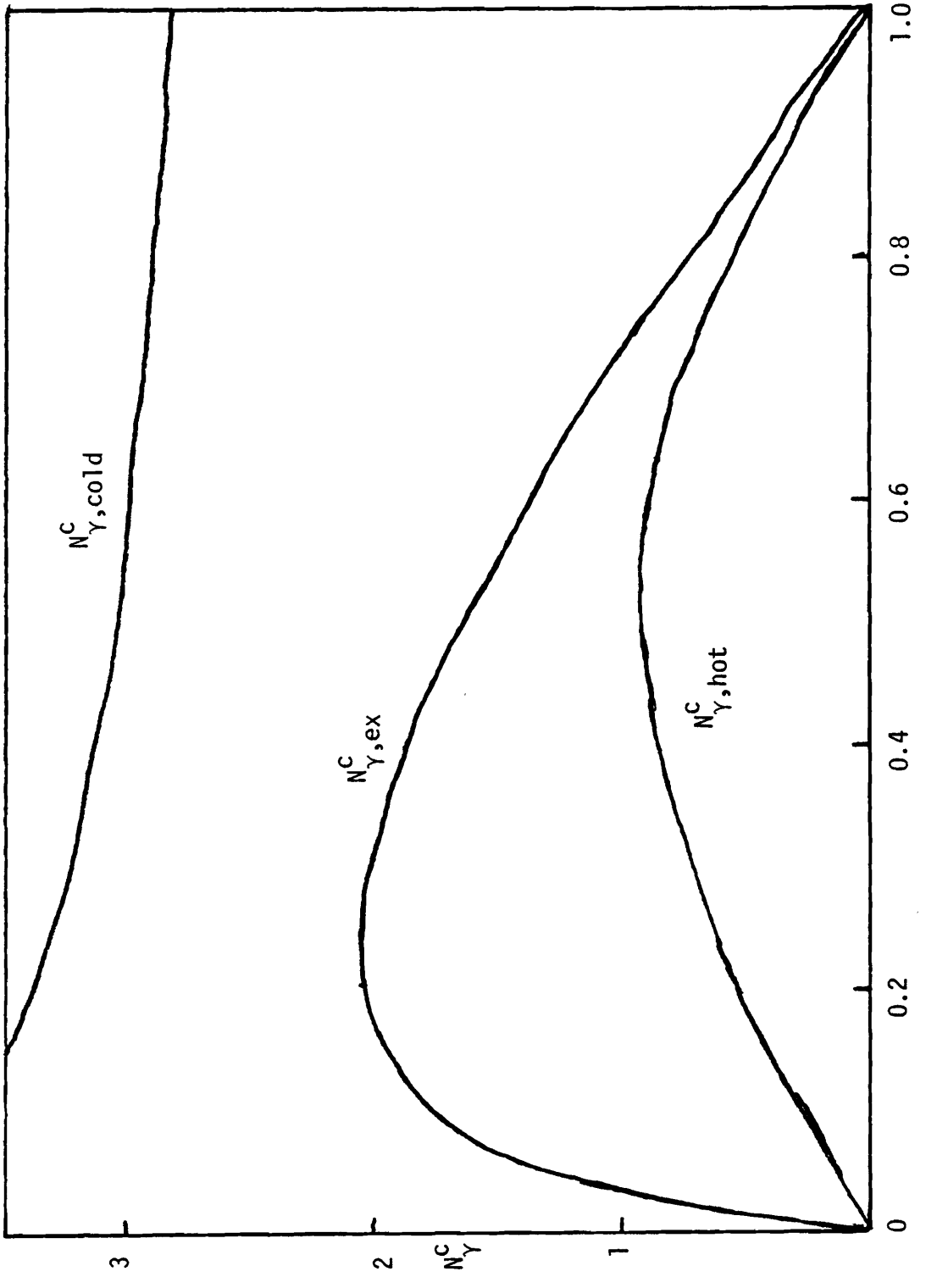

Figure 3

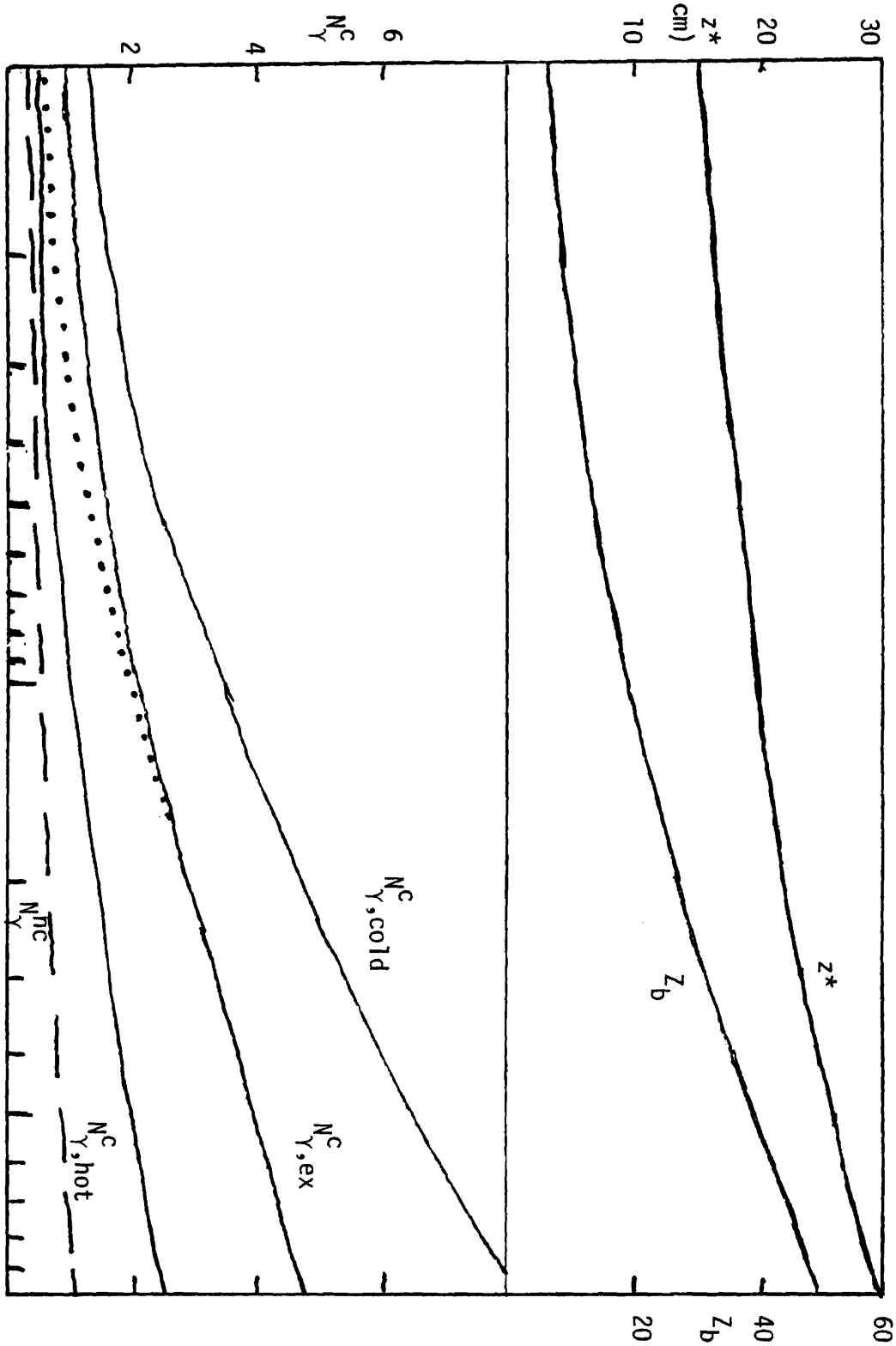
30
20
z* (cm)
10
6
N_γ^c
4
2
0.1
1.0
10
pressure (torr)
z*
Z_b
Z_b
60
40
20
$N_{\gamma,cold}^c$
$N_{\gamma,ex}^c$
$N_\gamma^{\overline{mc}}$
$N_{\gamma,hot}^c$

Figure 4